Proc. Natl. Acad. Sci. USA
Vol. 75, No. 4, pp. 1680–1684, April 1978
Biochemistry

Characterization of the histone core complex

(histone tetramer/histone octamer/equilibrium/crosslinking)

SU-YUN CHUNG†, WALTER E. HILL‡, AND PAUL DOTY†

† Department of Biochemistry and Molecular Biology, Harvard University, Cambridge, Massachusetts 02138; and ‡ Department of Chemistry, University of Montana, Missoula, Montana 59812

Contributed by Paul Doty, January 16, 1978

ABSTRACT **A stable histone core complex containing equimolar ratios of H2A, H2B, H3, and H4 has been isolated from chicken erythrocyte chromatin in high salt. This complex has been characterized by sedimentation and chemical crosslinking studies. In velocity ultracentrifugation, only one single sharp sedimentation boundary has been observed with sedimentation coefficient $S^0_{20,w} = 3.8 \pm 0.1$. The molecular weight of the histone core complex has been investigated by low-speed sedimentation equilibrium studies over a wide range of protein concentration. Analysis of the apparent weight-average molecular weight as a function of concentration indicates that the histone core complex in 2 M NaCl, pH 9.0, is in equilibrium between a tetramer (H2A)(H2B)(H3)(H4) and an octamer $[(H2A)(H2B)(H3)(H4)]_2$ species with a tetramer molecular weight of 55,000. The equilibrium constant K is approximately 1.2×10^{-5} liter per mol at 10°. Evidence of such a tetramer–octamer equilibrium in solution is also supported by the results of our chemical crosslinking experiments on the histone core complex.**

A well-characterized entity within the basic subunit of chromatin, the nucleosome, is the "core particle," which has a molecular weight of 200,000 and contains approximately 140 base pairs of DNA and two molecules each of the histones H2A, H2B, H3, and H4 (1, 2). Electron microscopy (3, 4), neutron scattering (5, 6), and x-ray diffraction (7) studies indicate that the "core particle" is a disk 110 Å wide by 55 Å high with two turns of DNA localized around the compact histone center. The arrangement of histones in the center and along the DNA within a nucleosome is not known. Proximity of certain histones within the nucleosome has been established by protein crosslinking studies; in particular, the use of zero-length crosslinking agents, ultraviolet light, tetranitromethane, and carbodiimide, has demonstrated close contact between H2B and H4, H2B and H2A, and H3 and H4, respectively (8, 9); furthermore, H2B is probably bound simultaneously to both H2A and H4 *in vivo* (8). Solution studies on mixtures of isolated histones have shown that histones H2A, H2B, H3, and H4 interact pairwise and that each possesses at least two distinct domains for interaction with other histones (9). Their interactions can be roughly divided into two categories: strong interactions between the pairs H2A-H2B, H2B-H4, and H3-H4, and weak interactions between the pairs H2A-H3, H2B-H3, and H2A-H4 (9). Along with dimeric complexes found in mixtures of histone pairs, the arginine-rich histones form a tetramer $[(H3)(H4)]_2$ (10–13). In addition, more complex oligomeric structures are found in solutions of high ionic strength (2 M NaCl) at neutral to alkaline pH (pH 7–10) after gentle extraction of the chromatin with high salt, although the precise nature of the oligomers is not clear (6, 14–17). The elevated ionic strength and pH reduce the repulsions between the highly charged histones, possibly providing an environment similar to that provided by DNA in the nucleosome. In fact, the configuration of the histone complex in high salt (but not in low salt) is at least very similar to that of histones in nucleosome (6, 14, 17), suggesting that the protein species present in the high salt solution is the histone core complex within nucleosomes. In view of the complexity of histone–histone interactions and the potential implications of the oligomeric structure of the histone core complex in the internal structure of the nucleosome, we have critically investigated the histone core complex at high ionic strength by physical and chemical techniques. We find that the histone core complex contains equimolar amounts of H2A, H2B, H3, and H4 and exists in a tetramer–octamer equilibrium with a tetramer molecular weight of 55,000.

The costs of publication of this article were defrayed in part by the payment of page charges. This article must therefore be hereby marked "advertisement" in accordance with 18 U. S. C. §1734 solely to indicate this fact.

MATERIALS AND METHODS

Preparation and Characterization of Histone Core Complex. Red blood cells were obtained from adult white Leghorn chickens and the nuclei were isolated according to Shaw *et al.* (18). The histone core complex was prepared at 4° by the method of Wooley *et al.* (17; personal communication). The purified nuclei were lysed against an excess of distilled water; the histones H1 and H5 and nonhistone proteins were removed from the chromatin by raising the salt to 0.6 M NaCl/10 mM sodium borate, pH 9.0. The chromatin was then pelleted at 24,000 rpm for 90 min in a Beckman 30 rotor. The pellet was washed twice in 0.6 M NaCl/10 mM sodium borate, pH 9.0, and centrifuged as before. The histone core complex was dissociated from DNA by adding NaCl to 2 M at pH 9.0 and isolated by pelleting the DNA at 45,000 rpm for 14 hr in a Beckman 65 rotor. Throughout the preparation, 0.1 mM phenylmethylsulfonyl fluoride was used to inhibit protease activity. The histone core complex was free of DNA, as indicated by an A_{230}/A_{260} ratio of 17–18, and was stable for more than a month stored at 4°. To determine the extinction coefficient of the histone core complex in 2 M NaCl, pH 9.0, we measured the absorption spectra in a Cary 118 spectrophotometer and determined the protein concentrations independently by both amino acid analysis (AAA Lab, Seattle, WA) and dry-weight measurement. Both methods yield an extinction coefficient of 4.2 ± 0.1 liter per g-cm at 230 nm.

Sedimentation Experiments. For sedimentation studies, all protein solutions were in dialysis equilibrium. The sedimentation experiments were performed in a Spinco model E analytical ultracentrifuge equipped with a photoelectric scanner. An ultraviolet absorption optical system and 12-mm double sector cells filled with solution and dialysate were routinely used. Absorbances of protein solutions across the ultracentrifuge cells were converted into concentrations in g/liter by multiplication by conversion factors, which were determined by measuring the absorbances of tryptophan solutions in a Cary 118 spectrophotometer and in the ultracentrifuge. In some experiments at high protein loading concentrations (>5 g/liter),

Abbreviation: CHES, cyclohexylaminoethane sulfonic acid.

both Rayleigh interference and schlieren optical systems were used in addition.

Sedimentation Equilibrium Analysis. For the analysis of a nonideal tetramer–octamer association, we followed a simple graphical procedure developed to evaluate the association constant and the second virial coefficient (19). From conservation of mass, the equilibrium constant K is described as $c = c_1 + Kc_1^2$ and $(1 - f_1)/f_1 = Kcf_1$, in which c is the total concentration, c_1 is the tetramer concentration, and $f_1 = c_1/c$ is the weight fraction tetramer. The apparent average molecular weights, M_{wc}^{app} and M_{nc}^{app}, are related to the true average molecular weights, M_{wc} and M_{nc}, by

$$M_1/M_{wc}^{app} = M_1/M_{wc} + B_1M_1c \quad [1]$$

$$M_1/M_{nc}^{app} = M_1/M_{nc} + B_1M_1c/2 \quad [2]$$

in which M_1 is the monomer molecular weight and M_{nc}^{app} is evaluated by trapezoidal numerical integration from the plot of M_{wc}^{app} against c following the definition $c/M_{nc}^{app} = \int_0^c dc/M_{wc}^{app}$ (20). The second virial coefficient B_1 can be eliminated from Eqs. 1 and 2 by introducing a new parameter

$$\xi = 2M_1/M_{nc}^{app} - M_1/M_{wc}^{app} = 2M_1/M_{nc} - M_1/M_{wc},$$
$$\text{or } \xi = (1 + f_1) - 1/(2 - f_1). \quad [3]$$

At a given concentration c, ξ can be obtained from the experimental data (M_{wc}^{app} and M_{nc}^{app}) and f_1 can be obtained as the solution to the quadratic Eq. 3. A plot of $(1 - f_1)/f_1$ against cf_1 should yield a straight line with the slope equal to the equilibrium constant K. The second virial coefficient B_1 can be obtained from the slope of the linear plot of $M_1/M_{wc}^{app} - 1/(2 - f_1)$ against c.

RESULTS

Composition and Stoichiometry of Histone Core Complex. The composition of the histone core complex, analyzed in polyacrylamide/urea gels, is shown in Fig. 1. Comparison of the densitometric tracings of the gels for the histone core complex and the total histone extract from erythrocyte nuclei indicates that histones H1 and H5 are completely absent in the histone core complex. The relative ratios of H2A, H2B, H3, and H4 obtained from the area under each resolved peak in Fig. 1 are identical for both gel tracings, indicating that the four histones are present in essentially equimolar quantities. Since it is well established that the four inner histones are present in equimolar ratio in nuclei (22), we conclude that the histone core complex isolated in this work consisted of histones H2A, H2B, H3, and H4 in equimolar ratio.

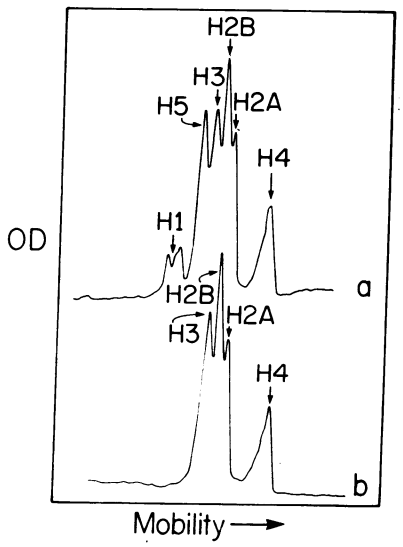

FIG. 1. Urea (2.5 M)/polyacrylamide (15%) gel electrophoresis of histones. (*a*) Total acid-extracted histones from chicken erythrocyte nuclei; (*b*) histone core complex. The tube gels were run according to Panyim and Chalkley (21), stained in 1% amido black, and scanned at 615 nm.

Apparent Specific Volume. In order to accurately evaluate the sedimentation coefficient $s_{20,w}$ and molecular weight of the histone core complex in 2 M NaCl/10 mM cyclohexylaminoethane sulfonic acid (CHES), pH 9.0, the apparent specific volume (ϕ^*) at constant chemical potential was determined experimentally. The protein solutions were prepared by exhaustive dialysis against the solvent.

The measured density of the histone core complex in 2 M NaCl/10 mM CHES, pH 9.0, as a function of protein concentration is presented in Fig. 2. The density increment $\partial\rho/\partial c$ obtained from the slope of a linear least-squares regression of the data points is 0.210. Substituting $\partial\rho/\partial c = 0.210$ and the measured solvent (dialysate) density ρ_0 into the expression (23), $\phi^* = (1 - \partial\rho/\partial c)/\rho_0$, yields an apparent specific volume of 0.730 ± 0.005 ml/g. This experimentally determined value is comparable to the values of $\bar{v} = 0.733$ (H3 and H4) and $\bar{v} = 0.732$ (H2A and H2B) which are estimated from the amino acid composition of calf thymus histones and corrected for the Donnan effect (24). In a similar manner, the apparent specific volume of the histone core complex in 1 M NaCl/10 mM CHES, pH 9.0 was determined to be 0.733 ± 0.005 ml/g.

Sedimentation Velocity. Boundary sedimentation velocity of the histone core complex in 2 M NaCl/10 mM CHES, pH 9.0, was measured at various protein concentrations (0.2–18 g/liter). A single symmetric sedimentation boundary was observed in all cases. A plot of $s_{20,w}$ as a function of concentration is shown in Fig. 3. Except at very low concentration, $s_{20,w}$ decreases very slightly with increasing concentration and extrapolates to $s^0_{20,w}$ of 3.8 ± 0.1.

The same sedimentation coefficient was obtained in the presence of magnesium ions (10–100 mM $MgCl_2$) and at pH 7.0. However, we observed that at low salt (1 M NaCl), low pH (pH 5.0), or low protein concentrations (<0.5 mg/ml), the sedimentation boundary broadened and the sedimentation coefficient, $s_{20,w}$, decreased, indicating partial dissociation. Moreover, rapidly sedimenting material, presumably aggregated histones, accompanied partial dissociation.

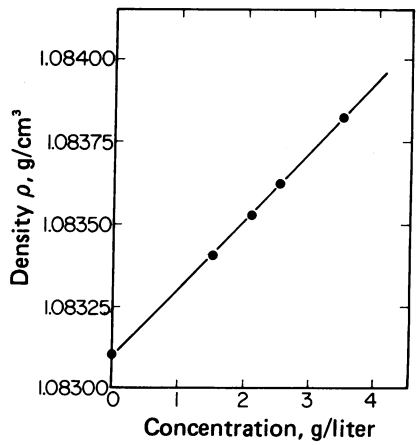

FIG. 2. Densities of the histone core complex in 2 M NaCl/10 mM CHES, pH 9.0. The densities were measured with a Digital Density Meter DMA-02C (Anton Paar, Graz, Austria). The instrument was calibrated against distilled water and KCl solutions of known density. The temperature was maintained at $4.000 \pm 0.003°$ by a precision temperature controller. The protein concentrations were determined spectrophotometrically.

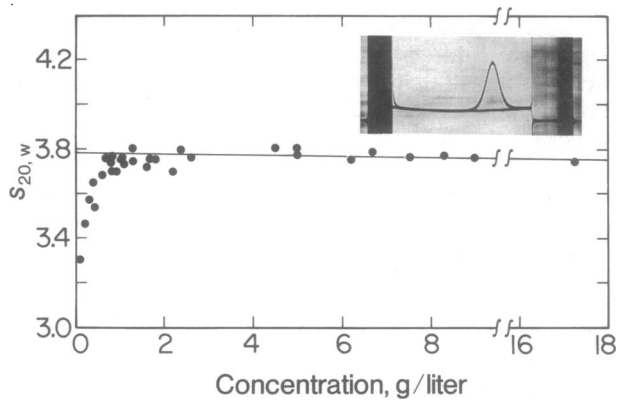

FIG. 3. Sedimentation velocity analysis of the histone core complex in 2 M NaCl/10 mM CHES, pH 9.0. (*Inset*) Typical schlieren pattern of the histone core complex. Experiments were at 20° with rotor speeds of 22,000–52,000 rpm.

Sedimentation Equilibrium. The results of low-speed sedimentation equilibrium studies of the histone core complex in 2 M NaCl/10 mM CHES, pH 9.0 are presented in Fig. 4. The plots of apparent weight-average molecular weight as functions of concentration from experiments with different initial loading concentrations (1–18 mg/ml) superimpose on a single curve; this suggests that the system is a single thermodynamic component. The single sharp boundary observed in sedimentation velocity experiments confirms that the system consists of one component in equilibrium with one or more multimers. The curve extrapolates at $c = 0$ to the "monomer" molecular weight M_1 of approximately 55,000. (The four histones H2A, H2B, H3, and H4 have a total molecular weight of 54,370.) The nature of the concentration dependence is consistent with dissociation at low concentrations and the display of nonideality at high concentrations.

The stoichiometry of this self-associating system was analyzed according to a "two-species plot" of Roark and Yphantis (19). We shall consider a "monomer" as the smallest molecular species that participates in the equilibrium. Because of its molecular weight, we assume this "monomer" to be the histone tetramer (H2A)(H2B)(H3)(H4) and the "dimer" to be the histone octamer $[(H2A)(H2B)(H3)(H4)]_2$. The plot of M_{wc}^{app}/M_1 against M_1/M_{nc}^{app} in Fig. 5 shows that the data from low concentrations fit into the standard "monomer–dimer" line and deviate negatively at high concentration due to nonideality. This deviation is in the opposite direction from that which would occur if more than two molecular species were present in the system. Thus, the results strongly suggest that at 2 M NaCl, pH 9.0, the histone tetramer (H2A)(H2B)(H3)(H4) exists in equilibrium with the octamer $[(H2A)(H2B)(H3)(H4)]_2$. The experimental data intersect the hyperbola ($M_{wc}/M_{nc} = 1$) at $M_1/M_{nc} = 1$. This confirms the monomer molecular weight assignment of 55,000 obtained from extrapolation in Fig. 4. The weight fraction of tetramer f_1 present at various concentrations calculated from Eq. 3 is summarized in Table 1, where it is shown that the tetramer is the predominant species at low protein concentration (<3 mg/ml). However, as the protein concentration increases, the octamer appears in increasing proportion: the weight fraction of tetramer drops to 27% at 15 mg/ml.

A graph of $(1 - f_1)/f_1$ against cf_1 is linear, indicating that only tetramer and octamer species are present in significant concentrations (19). From the slope of this linear plot, an equilibrium constant K of 0.68 liter/g is obtained. The plot of $M_1/M_{wc}^{app} - 1/(2 - f_1)$ against c also yields a straight line from which the nonideality term B_1M_1 can be evaluated; it is 0.014 liter/g.

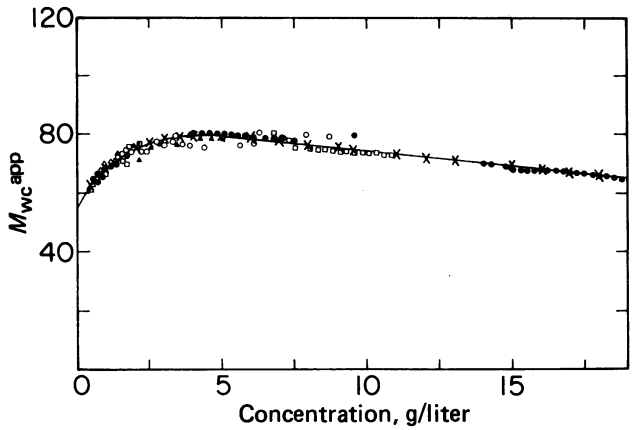

FIG. 4. Apparent weight-average molecular weight against protein concentration of histone core complex in 2 M NaCl/10 mM CHES, pH 9.0. M_{wc}^{app} from experiments at different initial loading concentration are shown by different symbols (○, ●, △, ▲, □). ×, Values of M_{wc}^{app} computed from the deduced equilibrium constant K (0.68) and the nonideality term B_1M_1 (0.014). The low-speed sedimentation equilibrium experiments were at 8766 rpm at 10° for 52–72 hr. The apparent weight-average molecular weight $M_{wc}^{app}(r)$, corresponding to concentration $c(r)$, was evaluated from the experimental data according to

$$M_{wc}^{app}(r) = \frac{2RT}{(1 - \bar{\nu}\rho)\omega^2} \frac{d\ln c}{d(r^2)}$$

in which c is the concentration in g/liter, R is the gas constant, T is the absolute temperature, $\bar{\nu}$ is the partial specific volume of the solute, ρ is the density of the solution, ω is the angular velocity, and r is the radial distance from the center of rotation. Each value $M_{wc}^{app}(r_0)$, the central point, was obtained by linear least-squares regression of five successive data points on the plot of $\ln c(r)$ against r^2.

The original assigned mode of association can be checked by calculating M_{wc}/M_1 and M_1/M_{nc} corrected for the nonideality by using $B_1M_1 = 0.014$. As shown in Fig. 5, the plot of M_{wc}/M_1 against M_1/M_{nc} falls exactly on the "monomer–dimer" lines over the concentration range studied. This confirms that the original assumption of a tetramer–octomer equilibrium is

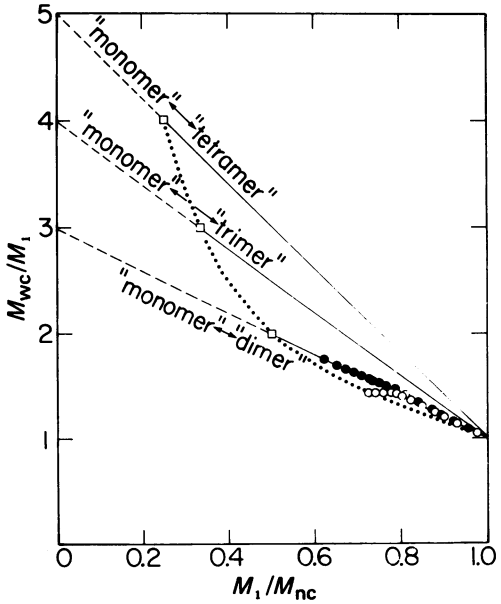

FIG. 5. "Two-species plot" of histone core complex: (○) M_{wc}^{app}/M_1 against M_1/M_{nc}^{app} and (●) M_{wc}/M_1 against M_1/M_{nc} after correction for nonideality. The dotted line represents the hyperbola $M_{wc}/M_{nc} = 1$.

Table 1. Weight fraction tetramer f_1 as a function of total protein concentration c in g/liter

c	0.25	0.5	1.0	2.0	3.0	4.0	5.0	10.0	15.0
f_1	0.91	0.84	0.73	0.59	0.50	0.44	0.41	0.33	0.27

correct. To visualize the fit of the experimental data to the two parameters K and B_1 obtained, we generate the function $M_{wc}^{app}(c)$ by reversing the computations, using $K = 0.68$ and $B_1M_1 = 0.014$. As shown in Fig. 4, the agreement between the experimental and the calculated apparent molecular weights over a wide concentration range (40-fold) is excellent. Moreover, the equilibrium constant K can be evaluated by an alternative method using the apparent equilibrium constant $K^{app} = M_1(M_{wc} - M_1)/c(2M_1 - M_{wc})^2$ without explicitly considering the nonideality (25). The intercept of the plot of K^{app} against c at $c = 0$ yields the quantity $K - B_1M_1$, from which a value of 0.60 liter/g for K is obtained in good agreement with the value previously determined.

In summary, low-speed sedimentation equilibrium studies show that the histone core complex in 2 M NaCl, pH 9.0, exists as a tetramer–octamer equilibrium with tetramer molecular weight of 55,000. The equilibrium constant for the association is roughly 0.68 liter/g or 1.2×10^{-5} liter/mol, and the second virial coefficient B_1 is 0.255×10^{-6} liter/g·dalton at 10°.

Crosslinking Experiments. A typical time course of crosslinking of histone core complex in 2 M NaCl/10 mM sodium borate, pH 9.0, followed by analysis in sodium dodecyl sulfate/5% polyacrylamide gel, is shown in Fig. 6. The gel patterns of the crosslinked proteins indicate that the rate of crosslinking is extremely fast. At 15 min, bands corresponding to monomer through octamer appear in the gel. After 1 hr, most crosslinked products are driven into the octamer and 12-mer bands, but the tetramer band is absent. The formation of higher oligomeric species is faster at increased protein or crosslinking reagent concentration. When the histone core complexes were crosslinked at low protein concentration (0.5 mg/ml), in which the tetramer is the predominant species, and at low dimethyl suberimidate concentration (0.1 mg/ml), bands corresponding to monomer, dimer, trimer, and tetramer were observed at 30 min (Fig. 6), suggesting that a stable tetramer exists at low protein concentration. However, as the reaction proceeds, higher oligomeric bands start to appear without a visible strong pause at the tetramer band. Thus, the crosslinking results are consistent with the existence of a tetramer–octamer equilibrium that is shifted toward the octamer by the chemical reaction.

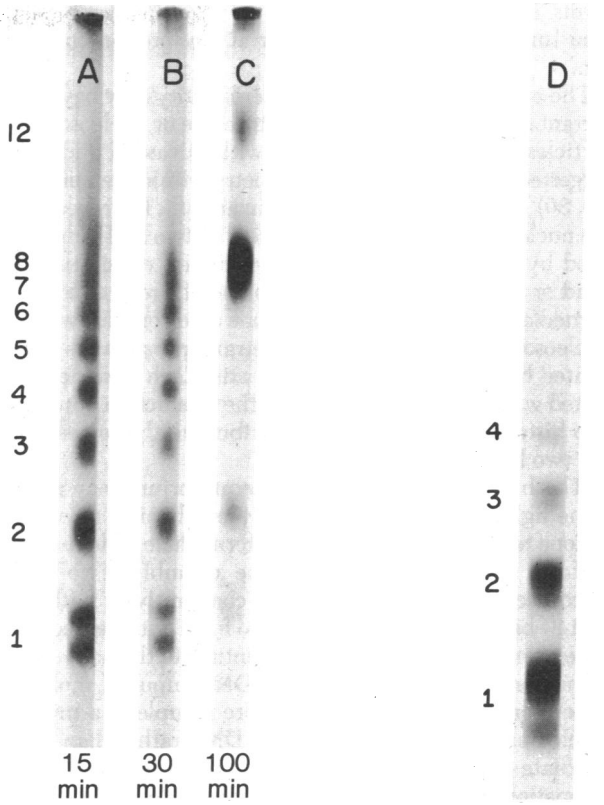

FIG. 6. Crosslinking of the histone core complex in 2 M NaCl/10 mM sodium borate, pH 9.0. (*A–C*) Crosslinking of the histone core complex at high protein concentration (3 mg/ml) with dimethyl suberimidate (1 mg/ml). (*D*) Crosslinking of the histone core complex at low concentration (0.5 mg/ml) with dimethyl suberimidate (0.1 mg/ml). The crosslinking procedure was that of Thomas and Kornberg (15) and 5% sodium dodecyl sulfate/polyacrylamide tube gels were run according to Davies and Stark (26). The molecular weights of the crosslinked products were calibrated against crosslinked aldolase (26) and histone monomers that were separately electrophoresed under identical conditions.

DISCUSSION

The low-speed sedimentation equilibrium studies demonstrate that the histone core complex in 2 M NaCl, pH 9.0, exists in equilibrium between a tetramer and an octamer species with appreciable solution nonideality. We have shown that a single set of values for the equilibrium constant K and the second virial coefficient B_1 is able to describe the association behavior of the histone core complex over a 40-fold range of protein concentration. The results strongly suggest that the equilibrium involves essentially only the tetramer and octamer species and that other oligomer intermediates, such as dimers and hexamers, cannot exist in any significant amount. The second virial coefficient B_1, 0.255×10^{-6} liter/g·dalton, found for this system is large, being of the order of 10–100 times greater than those generally found in the majority of buffered and supporting electrolyte–protein systems. Since the isoelectric point of the histone core complex is in the vicinity of pH 11.0 (27), the molecules are still highly charged at pH 9.0, leading to solution nonideality due to the Donnan effect. The large second virial coefficient explains the observation that the apparent weight-average molecular weight never approaches the octamer value of 110,000 in the concentration range studied (Fig. 3); this effect is also observed in other nonideal associating systems (28). The combined effects of nonideality and association, which affect the sedimentation coefficient in opposite directions, account for the near independence of $s_{20,w}$ of concentration. The crosslinking data offer independent confirmation of the proposed tetramer–octamer equilibrium in solution. However, the crosslinking reaction tends to drive the equilibrium toward the octamer. At low protein concentration, even though the major species in solution is a tetramer, the major crosslinked product is an octamer. This behavior illustrates the need for extreme care in the interpretation of crosslinking data for systems in equilibrium.

The histone core complex is homogeneous and we do not observe aggregates and dimers at concentrations above 0.5 mg/ml. Thus, tetrameric complexes other than the heterologous (H2A)(H2B)(H3)(H4) species probably do not exist in appreciable quantities in solution of the histone core complex since H3 and H4 are insoluble in 2 M NaCl and form heterogeneous aggregates whereas H2A and H2B form a dimer (14). Moreover, Weintraub *et al.* (14) have suggested that the histone core complex at pH 7.1 in 2 M NaCl is a heterologous tetramer (H2A)(H2B)(H3)(H4), a conclusion basically supported by our

results. In particular, at pH 7.1 the equilibrium may be shifted even further toward the tetramer at low protein concentration.

The existence of a stable tetrameric entity may have an important impltion for the internal structure of nucleosome core particles. Digestion experiments with DNases I and II have suggested that there is 2-fold symmetry within the nucleosome (29, 30). Recently, x-ray diffraction analysis has revealed that the nucleosome core particle consists of two half-subunits related by approximately mirror symmetry, consistent with a dyad or pseudo-dyad axis in the plane of projection (7). This immediately suggests that the histone core complex within the nucleosome is arranged as two tetrameric subunits that are related by a dyad or pseudo-dyad axis. Each tetramer is associated with one turn of DNA, and the interaction between the two histone tetramers might contribute to the forces holding the two loops of DNA together.

The histone tetramer–octamer equilibrium may also shed some light on the histone assembly mechanism *in vivo*. The histone tetramer may serve as an intermediate, able to dimerize to form an octamer during histone assembly. Two moles of histone core complex reconstitute cooperatively with 1 mole of 140-base-pair DNA fragments to form a stable nucleosome core particle that appears to be identical to the native nucleosome core particle (31). At high DNA input (1 mol of 140-base-pair DNA/mol of histone core complex), a mixture of nucleosome core particle and free DNA rather than an intermediate is found. These results are consistent with octamer formation being promoted by the presence of DNA. However, the reconstitution experiments do not reveal the mechanism and kinetics of histone assembly into nucleosomes. Recently, nucleosomal histones have been shown to assembly and segregate conservatively during chromosomal replication; thus, the new histones and old histones do not mix in forming a histone octamer in a nucleosome (32). This observation may also imply that during chromosomal replication and unwinding of nucleosomal DNA, the two tetramers remain intimately associated.

We thank Dr. K. E. Van Holde for helpful discussions. We also thank M. Smart for expert technical assistance. S.-Y.C. was supported by a National Institutes of Health postdoctoral fellowship. This research was supported in part by National Institutes of Health Grant HD-01229.

1. Van Holde, K. E., Shaw, B. R., Lohr, D., Herman, T. M. & Kovacic, R. T. (1975) *Fed. Eur. Biochem. Soc. Meet. 10th*, 57–72.
2. Noll, M. (1976) *Cell* **8**, 349–355.
3. Langmore, J. P. & Wooley, J. C. (1975) *Proc. Natl. Acad. Sci. USA* **72**, 2691–2695.
4. Wooley, J. C. & Langmore, J. P. (1977) in *Molecular Human Cytogenetics*, eds. Sparkes, R. S., Comings, D. J. & Fox, C. F. (Academic, New York), pp. 41–51.
5. Pardon, J. F., Worcester, D. L., Wooley, J. C., Tatchell, K., Van Holde, K. E. & Richard, B. M. (1975) *Nucleic Acids Res.* **2**, 2163–2176.
6. Pardon, J. F., Worcester, D. L., Wooley, J. C., Cotter, R. I., Lilley, D. M. J. & Richards, B. M. (1977) *Nucleic Acids Res.* **9**, 3199–3214.
7. Finch, J. T., Lutter, L. C., Rhodes, D., Brown, R. S., Ruchton, B., Levitt, M. & Klug, A. (1977) *Nature* **269**, 29–36.
8. Martinson, H. G. & McCarthy, B. J. (1976) *Biochemistry* **15**, 4126–4131.
9. Bonner, W. M. & Pollard, H. B. (1975) *Biochem. Biophys. Res. Commun.* **64**, 282–288.
10. D'Anna, J. A., Jr. & Isenberg, I. (1974) *Biochemistry* **13**, 4992–4997.
11. D'Anna, J. A., Jr. & Isenberg, I. (1974) *Biochem. Biophys. Res. Commun.* **61**, 343–347.
12. Roark, D. E., Geoghegan, T. E. & Keller, G. H. (1974) *Biochem. Biophys. Res. Commun.* **59**, 542–547.
13. Kornberg, R. D. & Thomas, J. O. (1974) *Science* **184**, 865–868.
14. Weintraub, H., Palter, K. & Van Lente, F. (1975) *Cell* **6**, 85–110.
15. Thomas, J. O. & Kornberg, R. D. (1975) *Proc. Natl. Acad. Sci. USA* **72**, 2626–2630.
16. Campbell, A. M. & Cotter, R. I. (1976) *FEBS Lett.* **70**, 209–211.
17. Wooley, J. C., Pardon, J. F., Richards, B. M., Worcester, D. L. & Campbell, A. M. (1977) *Fed. Proc. Fed. Am. Soc. Exp. Biol.* **36**, 810.
18. Shaw, B. R., Herman, T. M., Kovacic, R. T., Beaudreau, G. S. & Van Holde, K. E. (1976) *Proc. Natl. Acad. Sci. USA* **73**, 505–509.
19. Roark, D. E. & Yphantis, D. A. (1969) *Ann. N.Y. Acad. Sci.* **164**, 245–278.
20. Adams, E. T., Jr. (1965) *Biochemistry* **8**, 1646–1654.
21. Panyim, S. & Chalkley, R. (1969) *Arch. Biochem. Biophys.* **130**, 337–346.
22. Joffe, J., Keene, M. & Weintraub, H. (1977) *Biochemistry* **16**, 1236–1238.
23. Casassa, E. F. & Eisenberg, H. (1961) *J. Phys. Chem.* **65**, 427–433.
24. Roark, D. R., Geoghegan, T. E., Keller, G. H., Matter, K. V. & Engle, R. L. (1976) *Biochemistry* **15**, 3019–3025.
25. Adams, E. T., Jr. & Fujita, H. (1963) in *Ultracentrifugal Analysis in Theory and Experiment*, ed. Williams, J. W. (Academic, New York), pp. 119–129.
26. Davies, G. E. & Stark, G. R. (1970) *Proc. Natl. Acad. Sci. USA* **66**, 651–656.
27. Young, E. G. (1963) in *Comprehensive Biochemistry*, eds. Florkin, M. & Stotz, E. H. (Elsevier, New York), Vol. 7, p. 25.
28. Williams, J. W. (1972) *Ultracentrifugation of Macromolecules* (Academic, New York).
29. Simpson, R. T. & Whitlock, J. P., Jr. (1976) *Cell* **9**, 347–353.
30. Altenburger, W., Hörz, W. & Zachau, H. G. (1976) *Nature* **264**, 517–525.
31. Tatchell, K. & Van Holde, K. E. (1977) *Biochemistry* **16**, 5295–5303.
32. Leffak, I. M., Grainger, R. & Weintraub, H. (1977) *Cell* **12**, 837–845.